Period-doubling bifurcation readout for a Josephson qubit

Alexander B. Zorin
Physikalisch-Technische Bundesanstalt, Bundesallee 100, D-38116 Braunschweig, Germany and Skobeltsyn Institute of Nuclear Physics, Moscow State University, 119899 Moscow, Russia

Yuriy Makhlin
Landau Institute for Theoretical Physics, Kosygin st. 2, 119334 Moscow, Russia and Moscow Institute of Physics and Technology, 141700 Dolgoprudny, Russia

(Received 25 January 2011; revised manuscript received 13 April 2011; published 22 June 2011)

We propose a threshold detector with an operating principle based on a parametric period-doubling bifurcation in an externally pumped nonlinear resonance circuit. The ac-driven resonance circuit includes a dc-current–biased Josephson junction ensuring parametric frequency conversion (period-doubling bifurcation) due to its quadratic nonlinearity. A sharp onset of oscillations at the half-frequency of the drive allows for the detection of small variations of an effective inductance and, therefore, the readout of the quantum state of a coupled Josephson qubit. The bifurcation characteristics of this circuit are compared with those of the conventional Josephson bifurcation amplifier, and its possible advantages are discussed.

DOI: 10.1103/PhysRevB.83.224506 PACS number(s): 85.25.Cp, 74.50.+r, 05.70.Ln, 05.45.Gg

I. INTRODUCTION

The problem of an efficient readout of solid state quantum systems including Josephson qubits (see, e.g., Ref. 1) is of high importance from both theoretical and practical points of view. The dispersive readout techniques based on the radio-frequency measurement of reactive electrical parameters (for example, the Josephson inductance[2,3] or quantum Bloch capacitance[4,5]) received significant recognition since they allow one to minimize the backaction of the readout circuit on a Josephson qubit. Recently, particular interest has been focused on such systems operating in the nonlinear resonance regime (Duffing oscillator), which was possible due to a cubic nonlinearity of the supercurrent in a zero-phase biased Josephson junction.[6–9] In this regime, under the action of a weak signal and/or fluctuations, the circuit undergoes a bifurcation, that is, a transition between two stable oscillatory states.[10] The successful idea of the application of such a Josephson bifurcation amplifier (JBA) for the measurements of a qubit was first proposed by Siddiqi *et al*.[11] and developed in further works.[12,13] This success story has served for us as a motivation for the development of a readout based on another type of bifurcation in superconducting nonlinear circuits.

In this paper we propose a readout circuit whose operating principle is based on the excitation of half-harmonic oscillations, that is, a period doubling bifurcation (PDB). This striking phenomenon is a precursor of chaotic regime (manifesting itself in a cascade of PDBs) and may occur in an oscillating system like a force-driven pendulum or an ac-driven Josephson junction.[14] With only odd nonlinearity in the corresponding Duffing equation, PDB is suppressed.[15] However, additional even nonlinear terms, which arise for example when the Josephson junction is current biased below the critical value, makes double-period solutions possible and particularly suitable for detection. Physically the quadratic nonlinearity of reactance ensures parametric conversion of the drive down to the half-frequency (a parametric oscillator of the second kind according to classification given in Ref. 16). This is a complementary case to the parametrically driven system (parametric oscillator of the first kind[16]) where the pumping signal periodically modulates the (nonlinear) reactance[17] and can also cause the PDB effect. Technically this case can be realized, for example, by a periodic modulation of the critical current I_c of the zero–dc-biased Josephson element in a dc-SQUID configuration by using an alternating magnetic flux driving. This was recently done by Wilson *et al*. in the experiment on photon generation in a coplanar waveguide cavity incorporating such a parametrically pumped SQUID.[18] In our paper we focus, however, on a force-driven parametric oscillator of the second kind with quadratic Josephson nonlinearity, which enables PDB-based detection of small variations in the effective inductance, induced by a coupled circuit, for example, a Josephson qubit.

The essential difference of the PDB from the JBA regime consists of the parametric nature of the PDB resonance manifesting itself in abrupt switching from the zero-oscillation state to the dynamic state with a double period and an appreciable amplitude of the oscillations.[16] This regime may be favorable for an output-stage preamplifier receiving, in the case of the PDB, a signal with zero background. Moreover, as we shall show below, the switching characteristics of our circuits are somewhat different from those of conventional JBA; in particular, we find that in addition to better contrast between two possible stationary states of the PDBA, it may have a narrower switching region.

II. DYNAMICS OF THE CIRCUIT

The PDB circuit (see Fig. 1) comprises a dc-current–biased Josephson junction with the critical current I_c, capacitance C including the self-capacitance of the junction with, possibly, a contribution of an external capacitance, the linear shunting conductance G, as well as an attached qubit, presented here as a charge-phase qubit.[2,19] The circuit is driven by a harmonic signal $I_{ac} = I_A \cos 2\omega t$ at a frequency close to the double frequency of small-amplitude plasma oscillations ω_p, that is, $\omega \approx \omega_p$.

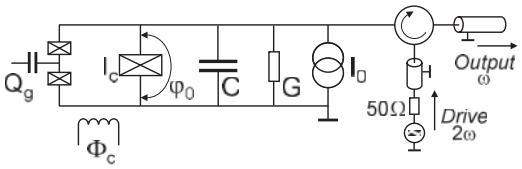

FIG. 1. Electric circuit diagram of the period-doubling–bifurcation detector with microwave-based readout. The resonator is formed by the inductance of a nonlinear Josephson junction (large crossed box), biased at a nonzero phase value φ_0, and the capacitance C. The linear losses are accounted for by the conductance G, which in a practical circuit is dominated by the matched microwave load. The resonator is coupled to a charge-phase qubit formed by a superconducting single-electron transistor with capacitive gate (left) and attached to the Josephson junction. The qubit operation at the optimal point for an arbitrary bias I_0 is ensured by a proper value of the external magnetic control flux Φ_c, applied to the qubit loop, and the gate charge Q_g on the qubit island.

Neglecting fluctuations, the dynamics of the bare system (excluding the qubit, whose quantum state only slightly changes the plasma frequency of the entire circuit, $\omega_p \to \widetilde{\omega}_p$) is governed by the model of a resistively shunted junction[20]:

$$\frac{\hbar C}{2e}\frac{d^2\varphi}{dt^2} + \frac{\hbar G}{2e}\frac{d\varphi}{dt} + I_c \sin\varphi = I_0 + I_{\rm ac}, \tag{1}$$

where the finite current bias $I_0 < I_c$ ensures a dc phase drop $\varphi_0 = \arcsin(I_0/I_c)$ across the Josephson junction. The small-ac-signal expansion ($x \ll 1$) of the Josephson supercurrent term includes the following components: $\sin\varphi = \sin(\varphi_0 + x) \approx \sin\varphi_0(1 - x^2/2 + x^4/24) + \cos\varphi_0(x - x^3/6)$. The angular frequency of small oscillations of φ around φ_0 is $\omega_p = (\cos\varphi_0)^{1/2}\omega_{p0}$, where the bare plasma frequency is $\omega_{p0} = (2eI_c/\hbar C)^{1/2}$.

Using the dot to denote derivatives with respect to the dimensionless time $\tau = \omega t$, we write the equation of motion for x in the following form:

$$\ddot{x} + x = \xi x - 2\theta\dot{x} + \beta x^2 + \gamma x^3 - \mu x^4 + 3P\cos 2\tau, \tag{2}$$

cf. the equation for a parametric oscillator of the first kind,[16,17] which includes the drive term $xP'\cos 2\tau$. The dimensionless coefficients in Eq. (2) are

$$\xi = 1 - \kappa, \quad |\xi| \ll 1, \quad \theta = G/2\omega C \equiv 1/2Q \ll 1, \tag{3}$$

$$\beta = 12\mu = (\kappa\tan\varphi_0)/2, \quad \gamma = \kappa/6, \quad 3P = \kappa I_A/I_c, \tag{4}$$

where $\kappa = (\omega_p/\omega)^2 \approx 1$ and Q is the quality factor. The quadratic nonlinear term ($\propto \beta$) in Eq. (2) ensures parametric down-conversion from the drive frequency 2ω.

The leading terms in the solution of Eq. (2) have the form $x \equiv y - P\cos 2\tau$, where $y(\tau)$ denotes oscillations at the frequency $\approx\omega$, and the second term is the forced oscillation at the drive frequency 2ω; $x(\tau)$ also contains other harmonics at multiple frequencies, which strongly influence its dynamics and stationary states,[21] cf. Eqs. (11) and (12) below. We apply the method of slowly varying amplitudes by introducing slow variables[16]:

$$y = A\cos(\tau - \alpha), \quad \dot{y} \approx -A\sin(\tau - \alpha). \tag{5}$$

The variables $A(\tau)$ and $\alpha(\tau)$ present the amplitude and phase (relative to the drive) of the oscillation at the half-frequency of the drive; they vary weakly over the period of these oscillations (with dimensionless rates $\ll 1$). Accordingly,

$$u = A\cos\alpha, \quad v = A\sin\alpha \tag{6}$$

are two quadratures of these oscillations, $u^2 + v^2 = A^2$. The dynamics of the slow variables is governed by the equations

$$\begin{pmatrix} \dot{A} \\ A\dot{\alpha} \end{pmatrix} = -\int_\tau^{\tau+2\pi} \frac{d\tau}{2\pi}\varepsilon F(x,\dot{x},\tau)\begin{pmatrix} \sin(\tau-\alpha) \\ \cos(\tau-\alpha) \end{pmatrix}, \tag{7}$$

with averaging over a 2π period of the oscillations at frequency ω (1 in dimensionless units), where the function in the integrand

$$\varepsilon F(x,\dot{x},\tau) = \xi x - 2\theta\dot{x} + \beta x^2 + \gamma x^3 - \mu x^4 \tag{8}$$

includes small terms at frequency ω and large terms at the drive frequency 2ω and its higher harmonics. The averaging over the period of oscillations in Eq. (7) yields a pair of reduced equations for the amplitude and the phase:

$$\dot{A} = -\theta A - \tfrac{1}{2}A\sin 2\alpha(\tilde{\beta}P - \tilde{\mu}PA^2), \tag{9}$$

$$\dot{\alpha} = \frac{\tilde{\xi}}{2} - \frac{\tilde{\beta}P}{2}\cos 2\alpha + \frac{3}{8}\tilde{\gamma}A^2 + \tilde{\mu}PA^2\cos 2\alpha. \tag{10}$$

The coefficients $\tilde{\xi}(P)$, $\tilde{\beta}(P)$, $\tilde{\gamma}(P)$, $\tilde{\mu}(P)$ to the leading order in P^2 are given by[21]

$$\tilde{\xi} = \xi, \quad \tilde{\beta} = \beta, \quad \tilde{\gamma} = \gamma + \tfrac{10}{9}\beta^2, \tag{11}$$

$$\tilde{\mu} = \mu - \tfrac{15}{16}\beta\gamma + \tfrac{7}{24}\beta^3, \tag{12}$$

which implies that $\tilde{\gamma} \approx (3 + 5\tan^2\varphi_0)/18$ and $\tilde{\mu} \approx (7/192)\tan\varphi_0(\tan^2\varphi_0 - 1)$. Corrections of order P^2 to these coefficients do not change further analysis qualitatively, but only slightly modify the results quantitatively.

III. STATIONARY SOLUTIONS, STABILITY, AND BIFURCATIONS

Equation (9) always has a trivial solution $A = 0$. In the limit of weak pumping ($P \ll 1$) and small resulting oscillations ($A^2 \ll 1$), the last terms ($\propto\tilde{\mu}P$) on the right-hand side of Eqs. (9) and (10) can be neglected, and the oscillation amplitude of the nonzero stationary solutions ($\dot{A} = \dot{\alpha} = 0$, $A \neq 0$) may be found explicitly[16]:

$$A_\pm^2 = \frac{4}{3\tilde{\gamma}}[-\tilde{\xi} \pm \sqrt{(\tilde{\beta}P)^2 - 4\theta^2}]. \tag{13}$$

For the pumping amplitude exceeding the threshold set by dissipation $|\tilde{\beta}P| > 2\theta$, the values

$$\tilde{\xi}_\pm = \pm\sqrt{(\tilde{\beta}P)^2 - 4\theta^2} \tag{14}$$

yield the range of frequency detunings, $\xi_- < \xi < \xi_+$, within which the zero solution is unstable. In this range the system switches into the oscillating state with a finite amplitude A_+ given by Eq. (13). For $\xi < \xi_-$ the parametric resonance curve

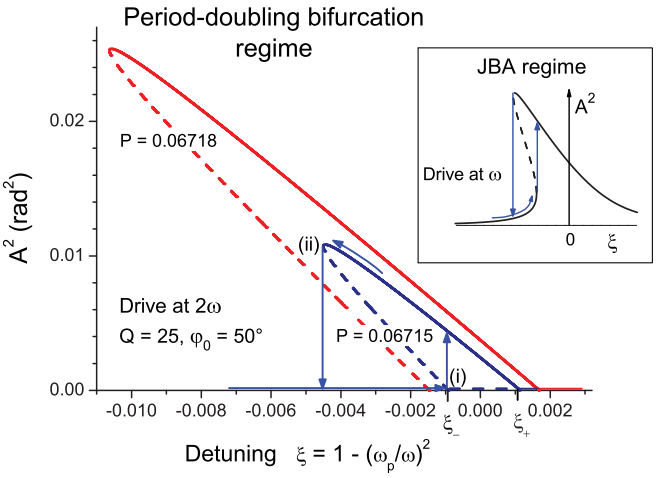

FIG. 2. (Color online) Intensity A^2 of oscillations of the Josephson phase at frequency ω versus frequency detuning ξ for two amplitudes of the pumping signal (at frequency 2ω). Dashed lines show unstable states. When the detuning approaches a bifurcation point [(i) or (ii)] PDB occurs (vertical arrows from or to the zero state, respectively). For comparison, a typical resonance curve of a JBA is sketched in the inset.

is multivalued with the stable trivial $A = 0$ and nontrivial A_+ solutions, while the solution A_- is unstable. Taking into account higher (e.g., $\propto\tilde{\mu}$) terms in Eqs. (9) and (10) ensures that $A_+(\xi)$ and $A_-(\xi)$ merge, limiting both the amplitude A_+ and the the range of bistability in ξ; for a stronger drive even higher nonlinearities become important. The shape of the resonance curve, calculated numerically from Eqs. (9) and (10), is shown in Fig. 2 for several values of the drive amplitude $3P$ just above the excitation threshold. However, for further considerations of the threshold behavior the higher nonlinearities are not crucial, and below we neglect the $\tilde{\mu}$ terms.

The stability diagram of the system in the space of the control parameters, the detuning $\tilde{\xi}$ and the driving amplitude P is shown in Fig. 3. The parameter plane is divided into three regions, with the following stable-state amplitudes [cf. Eq. (13)]: $A = 0$ in the lower region, A_+ in the upper region, and both 0 and A_+ in the "bistable" sector (this region is limited by two solid lines). The bifurcation lines are given by the relations $A_+ = A_-$ (lower left horizontal solid line), $A_- = 0$ [i.e., $\xi = \xi_-(P)$, upper solid curve], and $A_+ = 0$ [i.e., $\xi = \xi_+(P)$, dashed curve]. The coordinates of the triple point are $\xi = 0$ and $P = 2\theta/\tilde{\beta} \approx 2/(Q\tan\varphi_0)$.

Equations for the quadrature components of the velocity field,

$$\mathbf{v} = \begin{pmatrix} \dot{u} \\ \dot{v} \end{pmatrix} = \begin{pmatrix} \dot{A}\cos\alpha - A\dot{\alpha}\sin\alpha \\ \dot{A}\sin\alpha + A\dot{\alpha}\cos\alpha \end{pmatrix}, \tag{15}$$

where $\dot{A}$ and $\dot{\alpha}$ are given by Eqs. (9) and (10) can be represented as Hamiltonian equations of motion with friction:

$$\dot{u} = -\partial_v H - \theta u, \quad \dot{v} = \partial_u H - \theta v, \tag{16}$$

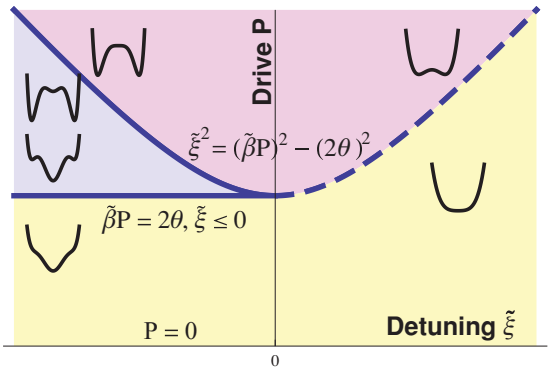

FIG. 3. (Color online) Stability diagram of the period-doubling–bifurcation readout. Stationary oscillatory solutions appear and disappear as the detuning ξ and driving amplitude P are varied. This is indicated by the sketched potential curves which show stable (minima) and unstable (maxima) states. The former include only the zero solution in the lower region, only a pair of equal-amplitude solutions A_+, A_+^* with a π phase shift in the upper region, and the zero and the pair A_+, A_+^* in the left, "bistable" sector-shaped region. The equations in the figure describe the bifurcation boundaries.

or, equivalently,

$$\dot{A} = -\theta A - \frac{1}{A}\partial_\alpha H, \quad A\dot{\alpha} = \partial_A H, \tag{17}$$

where the Hamiltonian is given by

$$H = (\tilde{\xi} - \tilde{\beta}P\cos 2\alpha)\frac{A^2}{4} + \frac{3}{32}\tilde{\gamma}A^4. \tag{18}$$

This Hamiltonian for the slow variables can be obtained from the Hamiltonian for the physical quantities.[21] Figure 4 shows a contour plot of the absolute value of the velocity $|\mathbf{v}| = (\dot{u}^2 + \dot{v}^2)^{1/2} = (\dot{A}^2 + A^2\dot{\alpha}^2)^{1/2}$ in the case of a multivalued stationary solution. One can see the darker S-shaped narrow

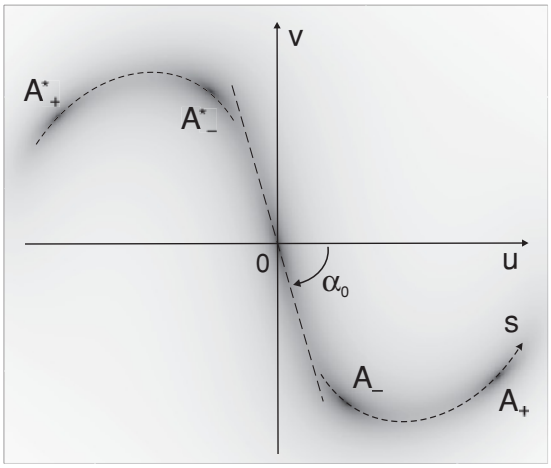

FIG. 4. Contour velocity plot calculated from Eqs. (9), (10), and (15) for the parameters corresponding to a multivalued solution. The absolute value of velocity $|\mathbf{v}|$ is lower in darker areas. The curvilinear trajectory along the valley of minimal velocity (short-dash line) is parametrized by s (cf. the straight line trajectory, predicted[17] and observed[18] in the parametrically pumped circuit). The straight dashed line at the origin indicates the most probable direction of escape from the zero state close to the bifurcation.

valley, where the motion is slow along the curvilinear s axis. The black spots in this area show the stationary solutions, which are the stable focus at zero, $A = 0$, the stable foci A_+ and A_+^* corresponding to equal-amplitude oscillations with a mutual phase shift of π, and the unstable saddles A_- and A_-^* (also with a mutual π shift). For weak dissipation these "saddle points" are the lower points of the barriers separating the basins of attraction of the foci in the landscape of H. Thus, the most probable escape path from the zero state is along the S-shaped valley.

In the vicinity of the bifurcation point ξ_- within the bistable region, the height of the energy barriers is small, and one can show that there is a separation of time scales, which can be used to solve the dynamics: the fast relaxation from the exterior points toward the S-shaped valley is followed by slow dynamics along the valley. In this region the points A_- and A_-^* are close to the origin, $u = v = 0$, and the slope α_0 of the valley at the origin can be found from Eq. (9):

$$\sin 2\alpha_0 = -\eta^{-1}, \quad \text{where} \quad \eta = \tilde{\beta} P/2\theta. \tag{19}$$

To describe the slow motion along the valley near the origin, where one can use the amplitude A as a coordinate, we first solve an equation for the fast motion in the axial α direction (variable α relaxes fast, with a typical rate of θ). To find the subleading nonlinear terms in the equation of motion along the valley, one needs to take into account the deviation of the valley near the origin from a straight line. The resulting equation of motion can be represented in the form of an easily solvable 1D equation (cf. Ref. 10):

$$\frac{ds}{d\tau} = -\frac{dW(s)}{ds}, \tag{20}$$

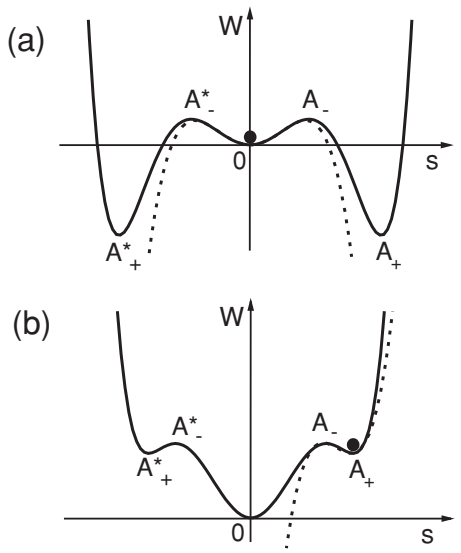

FIG. 5. A sketch of the potential $W(s)$ along the S-shaped region (see Fig. 4) for two ultimate cases: (a) bifurcation $0 \to A_+$ (A_+^*) (near the upper solid line in Fig. 3) and (b) bifurcation $A_+ \to 0$ (near the lower solid line in Fig. 3). Near the bifurcations, the dashed lines approximate the energy barriers by a quartic and a cubic polynomial, respectively.

where the pseudopotential is to the lowest orders a biquadratic polynomial $W = as^2 - bs^4$, where

$$a = -\frac{\delta\tilde{\xi}}{4}\sqrt{\eta^2 - 1}\,, \quad b = \frac{3}{32}\tilde{\gamma}\sqrt{\eta^2 - 1}\,. \tag{21}$$

For $\xi < \xi_-$ ($\delta\xi < 0$) one finds that $a > 0$. Thus, when ξ crosses ξ_- from above, the zero unstable stationary solution bifurcates and separates into a stable solution at zero and two symmetric unstable solutions A_- (Fig. 5). This property makes it sensitive to small changes in the circuit parameters (in particular to the qubit state via its effective Josephson inductance, which modifies the detuning ξ). The switching characteristics of such a detector can be found from the analysis of this system in the presence of noise, which results in a finite width of the transition. To describe the bifurcation-based readout, one needs to find the tunneling rate out of the shallow well $W(s)$ near the bifurcation.

IV. SWITCHING BETWEEN STATIONARY STATES

Small fluctuations due to the conductance G are taken into account by adding a noise term δI, with the spectral density $S_I(\omega) = 2\hbar\omega G \coth\frac{\hbar\omega}{2k_BT}$, to the right-hand side of Eq. (1). This gives rise to independent fluctuations of the two quadratures. Their correlation functions are

$$\langle \delta u(\tau)\delta u(\tau')\rangle = \langle \delta v(\tau)\delta v(\tau')\rangle = 2T_{\text{eff}}\delta(\tau - \tau'), \tag{22}$$

with $\langle \delta u(\tau)\delta v(\tau')\rangle = 0$ or

$$\langle \delta A(\tau)\delta A(\tau')\rangle = A^2\langle \delta\alpha(\tau)\delta\alpha(\tau')\rangle = 2T_{\text{eff}}\delta(\tau - \tau'), \tag{23}$$

with $\langle \delta A(\tau)\delta\alpha(\tau')\rangle = 0$, where the effective temperature

$$T_{\text{eff}} = \frac{\kappa^2 S_I(\omega)\omega}{8(I_c\cos\varphi_0)^2} \xrightarrow{\text{low}-\omega} \frac{\kappa^2 k_B T G\omega}{2(I_c\cos\varphi_0)^2}, \tag{24}$$

and the latter expression holds in the low-frequency (classical) limit $\hbar\omega \ll k_BT$. Upon the reduction to the 1D equation (20), this causes fluctuations with the same noise power,

$$\langle \delta s(\tau)\delta s(\tau')\rangle = 2T_{\text{eff}}\delta(\tau - \tau'), \tag{25}$$

which affect the motion along the s coordinate.

Adding the Langevin term $\delta s(\tau)$ on the right-hand side of Eq. (20), one can derive and then solve a 1D Fokker-Planck equation[10] [in fact, a Smoluchowski equation since the "mass" term $\propto d^2s/d\tau^2$ is absent in Eq. (20)] for the probability density $w(s,t)$ to find the system at point s at time t:

$$\frac{\partial w}{\partial t} = \frac{\partial}{\partial s}\left[\frac{\partial W(s)}{\partial s}w\right] + T_{\text{eff}}\frac{\partial^2 w}{\partial s^2}. \tag{26}$$

The escape rate out of the zero metastable state $A = 0$ to the stable state A_+ or A_+^* is given by Kramers' formula[22] reflecting the activational behavior of the system,

$$\Gamma = 2(\omega_A/2\pi)e^{-\Delta W/T_{\text{eff}}}\,, \tag{27}$$

where factor 2 accounts for two escape possibilities (to the left or right wells). For the overdamped case of a zero-mass particle, the formula for ω_A is given, for example, in Ref. 23. The prefactor ω_A is determined by the geometrical mean of

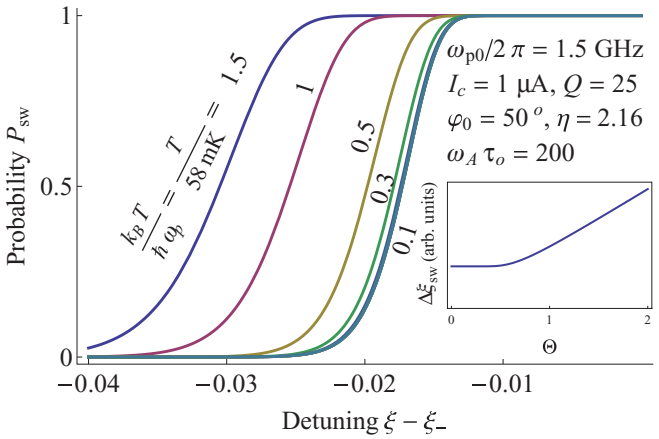

FIG. 6. (Color online) Switching curves for the period-doubling–bifurcation readout at various temperatures. Note saturation at low T, governed by "quantum noise" at $k_B T \lesssim \hbar\omega$. *Inset*: low-$T$ saturation, illustrated by the curves' width $\delta\xi_{sw}$ [inverse slope at $P = 0.5$, $\propto\sqrt{S(\omega)}$] as a function of $\Theta \equiv \sqrt{k_B T/\hbar\omega}$.

the curvatures of $W(s)$ at the bottom of the central well (equal to $2a$) and at the top of the barrier (equal to $4a$), that is,

$$\omega_A = 2\sqrt{2}a\omega = \omega\frac{|\delta\xi|}{\sqrt{2}}\sqrt{\eta^2 - 1}. \tag{28}$$

The barrier height to the lowest order in $\delta\xi = \xi - \xi_-$ is

$$\Delta W = a^2/4b \propto (\xi - \xi_-)^2. \tag{29}$$

Typical switching curves (switching probability $P_{sw} = 1 - e^{-\Gamma\tau_o}$ during some observation time τ_o vs ξ) are shown in Fig. 6 for various temperatures for a set of typical circuit parameters. Note that the position and the width of the switching curve (see inset) are saturated at low temperatures. This effect is not a manifestation of the real quantum tunneling, but is rather linked to the fact that activation in the rotating frame of the first harmonic [Eqs. (5) and (6)], that is, the low-frequency noise in that frame, is given in the laboratory frame by the noise at a finite frequency ω [cf. Eq. (24) and above].

Equation (29) implies that the width (along the detuning axis ξ) of the switching curves, given by the inverse slope $(dP/d\xi)^{-1}$ at $P = 0.5$, scales as $\delta\xi_{sw} \propto \sqrt{T}$ above saturation. Thus as $T \to 0$, it falls off slightly slower than that for the "standard" Josephson bifurcation amplifier,[11,24] where $\delta\xi_{sw} \propto T^{2/3}$. This (minor) difference stems from the symmetry of the PDBA with respect to a shift by a drive period: $\alpha \to \alpha + \pi$. This symmetry implies that the generic form of the 1D potential W near the bifurcation is $\varepsilon s^2 - as^4$, unlike $\varepsilon s - as^3$ for the JBA. Here ε measures the distance from the bifurcation and s is the relevant coordinate in phase space. However, this symmetry can be broken, and the stronger effect of cooling ($\delta\xi_{sw} \propto T^{2/3}$) restored by a weak admixture at frequency ω to the drive signal. An alternative strategy consists in using another bifurcation point, where $A_+ = A_-$ in Fig. 2 (on lowering the detuning ξ, the system follows the solution A_+ until it merges with A_-, where it switches abruptly to zero; there is no symmetry around this point).

V. DISCUSSION

Thus we have suggested two protocols of operation of the PDBA (with potentials shown in Fig. 5 and operation indicated by arrows in the parametric resonance plot, Fig. 2): one of them involves switching from the zero state to a large-amplitude stable state A_+ near the bifurcation point ξ_-, and the other involves a reverse switching from the large-amplitude state A_+ to zero near the merging point of A_+ and A_-. Note that in both cases to perform a readout, that is to find out if a switching has occurred, one needs to distinguish a zero state from a large-amplitude state. This should be contrasted with the JBA, where two finite-amplitude (and often, similar-amplitude, but different-phase) states have to be distinguished. From this viewpoint, the PDBA may be more convenient in practical applications. Other protocols can also be discussed (cf. Ref. 25).

The readout of a coupled qubit is based on the shift in the plasma frequency (and thus of the switching curve) due to different Josephson inductances in two qubit states. The inductance values depend on the type of qubit and its parameters. Generally the expected backaction of the PDBA readout on a qubit is similar to that of the JBA readout, that is, extremely low, and similar methods may be used in order to suppress it further and to improve fidelity (cf. Ref. 13). In both cases one source of such backaction is the near-equilibrium noise of the resistance, mostly that of a matched microwave load, which can be efficiently thermalized at the lowest stage of a fridge.[6] Due to the resonance impedance of both circuits, the noise components at the qubit Larmor frequency are suppressed, which reduces the rate of possible energy relaxation. Furthermore, a lower oscillation amplitude is desirable since modulation of the qubit level splitting by the resonator may lead to level crossings with spurious fluctuators.[6] The amplitude of the Josephson phase oscillations at the drive frequency 2ω in the PDBA is sufficiently small, $P \gtrsim 2\theta/\tilde{\beta} \sim Q^{-1}$, whereas oscillations at frequency ω are either absent (in the zero state) or have an amplitude comparable to that in the oscillating states of the JBA. The former property may be advantageous, for example, for QND[26,27] and single-shot[13] measurements of the quartic phase qubit.[28] Indeed, as was shown in Ref. 28, the effective Josephson inductance of this qubit is negative in both ground and excited states with the smaller absolute value in the excited state. Therefore, in contrast to the charge qubit, a magnetically coupled quartic qubit (see Fig. 1(a) in Ref. 28) should cause, in the excited state, a smaller shift of the resonance toward lower frequencies than in the ground state. In this case one can adjust the bifurcation threshold such that only the ground state induces the PDB, whereas at reading out of the excited state the PDB does not occur, and the qubit experiences only very weak oscillations of phase at frequency 2ω.

During the readout, the qubit state is encoded in the resulting oscillations of the PDBA by tuning the control parameters (such as the drive frequency and amplitude, i.e., ξ and P) to a point with the maximum difference (contrast) between the two switching curves. High contrast is reached when the shift in the plasma frequency exceeds the width of the switching curve. In an ideal arrangement this contrast reaches 100%: $P_{sw} = 0$ and 1 for two qubit states. For the

PDBA, the contrast reaches values comparable to those for the JBA with similar circuit parameters (for example, about 0.3% in frequency sensitivity for the parameters of Fig. 6 at low T that is sufficient for reliable readout of the charge-phase qubit[6] shown in Fig. 1). Further optimization of the PDBA parameters is possible.

Let us compare the switching curves for the PDBA and JBA[6] near the upper critical lines of the bistability region ($\eta_\uparrow$ in the notations of Ref. 6). We consider the tunneling exponents as functions of the dimensionless deviation of the drive amplitude from the bifurcation $1 - P/P_-$ for the PDBA, and we use the same notation, instead of $1 - \eta/\eta_\uparrow$, for the JBA. According to Refs. 24 and 6 for the JBA

$$\left|1 - \frac{P}{P_-}\right| \sim \left(\frac{k_B T}{E_J|\xi|}\right)^{2/3}. \tag{30}$$

For the PDBA we replace the difference $(\xi - \xi_-)$ in Eq. (29) by $\partial_P \xi_-(P_- - P)$. Assuming that the detuning $\xi \gtrsim 1$ (that is, $\delta\omega \gtrsim \omega/Q$), we find that the tunneling exponent is of the order

$$\frac{\Delta W}{T_{\text{eff}}} \approx Q^2 \frac{6\tilde{\gamma}\cos\varphi_0 E_J}{k_B T}|\xi|^3 \left(1 - \frac{P}{P_-}\right)^2. \tag{31}$$

Thus, increasing the detuning [and the corresponding driving amplitude $P_-(\xi)$] can suppress the width of the relevant switching curve (switching probability vs drive amplitude P):

$$\left|1 - \frac{P}{P_-}\right| \sim \left(\frac{k_B T}{E_J|\xi|}\frac{1}{Q^2|\xi|^2}\frac{1}{6\tilde{\gamma}\cos\varphi_0}\right)^{1/2}. \tag{32}$$

We note that various operation protocols of the readout device based on PDBA are possible, and one can force a crossing of the bifurcation region and a switching between the oscillating states by tuning various parameters. In particular, the current bias I_0, the amplitude, and frequency of the drive can be used for engineering a metapotential of desired shape and, therefore, optimization of the readout. In our analysis we have focused on the noise-induced activation over the barrier in this metapotential. As was shown [cf. above Eq. (24)] the effective "temperature" is set by the noise level at frequency ω and saturates on lowering the temperature T below $\hbar\omega/k_B$. This low-T regime may also be thought of as "quantum activation."[9,25,29] One could also consider the quantum tunneling.[30] However, in similar systems the corresponding tunneling rate is exponentially small, especially close to the bifurcation point (cf. Refs. 25 and 29).

VI. CONCLUSION

We have suggested the use of a nonlinear Josephson resonator—driven near its double plasma frequency—as a sensitive quantum detector. In this regime the system may develop a bifurcation with two possible stable states; it may be manipulated to force it to the state, correlated with the state of a coupled qubit. In contrast to the Josephson bifurcation amplifier, one of these states has a zero amplitude, which simplifies the task of resolving the two states. Furthermore, the properties of the detector are different from those of the JBA for similar parameters. In particular, the switching curve may be narrower than that of a JBA, which may result in a higher fidelity of the qubit readout. We note also that unlike the JBA, in the case of the PDBA the switching from the zero state is not affected by dephasing (including noise of the drive frequency) to the leading order.[25]

ACKNOWLEDGMENTS

We thank Michael Wulf, Ralf Dolata, and members of the Cluster of Excellence QUEST for useful discussions, as well as Yuli Nazarov and Mark Dykman for valuable comments. This work was partially supported by the EU through the EuroSQIP and SCOPE project, which acknowledges the financial support of the Future and Emerging Technologies (FET) programme within the Seventh Framework Programme for Research of the European Commission, under FET-Open Grant No. 218783, by DFG (German Science Foundation) through the Grant ZO124/2-1, by RFBR under Grant No. 09-02-12282-ofi_m, MES of RF, and the Dynasty foundation (YM).

[1] Yu. Makhlin, G. Schön, and A. Shnirman, Rev. Mod. Phys. **73**, 357 (2001).
[2] A. B. Zorin, Phys. Rev. Lett. **86**, 3388 (2001); Physica C (Amsterdam) **368**, 284 (2002); Zh. Eksp. Teor. Fiz. **125**, 1423 (2004) [Sov. Phys. JETP **98**, 1250 (2004)].
[3] A. Lupaşcu, C. J. M. Verwijs, R. N. Schouten, C. J. P. M. Harmans, and J. E. Mooij, Phys. Rev. Lett. **93**, 177006 (2004).
[4] M. A. Sillanpää, T. Lehtinen, A. Paila, Yu. Makhlin, L. Roschier, and P. J. Hakonen, Phys. Rev. Lett. **95**, 206806 (2005).
[5] T. Duty, G. Johansson, K. Bladh, D. Gunnarsson, C. Wilson, and P. Delsing, Phys. Rev. Lett. **95**, 206807 (2005).
[6] G. Ithier, Ph.D. thesis, Université Paris 6, 2005.
[7] I. Siddiqi, R. Vijay, M. Metcalfe, E. Boaknin, L. Frunzio, R. J. Schoelkopf, and M. H. Devoret, Phys. Rev. B **73**, 054510 (2006).
[8] A. Lupaşcu, E. F. C. Driessen, L. Roschier, C. J. P. M. Harmans, and J. E. Mooij, Phys. Rev. Lett. **96**, 127003 (2006).
[9] R. Vijay, M. H. Devoret, and I. Siddiqi, Rev. Sci. Instrum. **80**, 111101 (2009).
[10] M. I. Dykman and M. A. Krivoglaz, Physica A **104**, 480 (1980).
[11] I. Siddiqi, R. Vijay, F. Pierre, C. M. Wilson, M. Metcalfe, C. Rigetti, L. Frunzio, and M. H. Devoret, Phys. Rev. Lett. **93**, 207002 (2004).
[12] M. B. Metcalfe, E. Boaknin, V. Manucharyan, R. Vijay, I. Siddiqi, C. Rigetti, L. Frunzio, R. J. Schoelkopf, and M. H. Devoret, Phys. Rev. B **76**, 174516 (2007).
[13] F. Mallet, F. R. Ong, A. Palacios-Laloy, F. Nguyen, P. Bertet, D. Vion, and D. Esteve, Nat. Phys. **5**, 791 (2009).
[14] B. A. Huberman and J. P. Crutchfield, Phys. Rev. Lett. **43**, 1743 (1979); B. A. Huberman, J. P. Crutchfield, and N. H. Packard, Appl. Phys. Lett. **37**, 750 (1980).
[15] K. Wiesenfeld, E. Knobloch, R. F. Miracky, and J. Clarke, Phys. Rev. A **29**, 2102 (1984).

[16]V. Migulin, V. Medvedev, E. Mustel, and V. Parygin, in *Basic Theory of Oscillations*, edited by V. Migulin (Mir, Moscow, 1983).
[17]M. I. Dykman, C. M. Maloney, V. N. Smelyanskiy, and M. Silverstein, Phys. Rev. E **57**, 5202 (1998).
[18]C. M. Wilson, T. Duty, M. Sandberg, F. Persson, V. Shumeiko, and P. Delsing, Phys. Rev. Lett. **105**, 233907 (2010).
[19]D. Vion, A. Aassime, A. Cottet, P. Joyez, H. Pothier, C. Urbina, D. Esteve, and M. H. Devoret, Science **296**, 886 (2002).
[20]D. E. McCumber, J. Appl. Phys. **39**, 3113 (1968); W. C. Stewart, Appl. Phys. Lett. **12**, 277 (1968).
[21]B. G. Shteynas, Yu. Makhlin, and A. B. Zorin, in preparation.
[22]H. A. Kramers, Physica **7**, 284 (1940).
[23]V. I. Mel'nikov, Phys. Rep. **209**, 1 (1991).
[24]I. Siddiqi, R. Vijay, F. Pierre, C. M. Wilson, L. Frunzio, M. Metcalfe, C. Rigetti, and M. H. Devoret, in *Quantum Computation in Solid State Systems*, edited by B. Ruggiero, P. Delsing, C. Granata, Y. Pashkin, and P. Silvestrini (Springer, Berlin, 2006), p. 28.
[25]M. I. Dykman, *Applications of Nonlinear Dynamics: Model and Design of Complex Systems* (Springer, Berlin, 2009), p. 367.
[26]A. Lupaşcu, S. Saito, T. Picot, P. C. D. Groot, C. J. P. M. Harmans, and J. E. Mooij, Nat. Phys. **3**, 119 (2007).
[27]N. Boulant, G. Ithier, P. Meeson, F. Nguyen, D. Vion, D. Esteve, I. Siddiqi, R. Vijay, C. Rigetti, F. Pierre, and M. Devoret, Phys. Rev. B **76**, 014525 (2007).
[28]A. B. Zorin and F. Chiarello, Phys. Rev. B **80**, 214535 (2009).
[29]M. Marthaler and M. I. Dykman, Phys. Rev. A **73**, 042108 (2006).
[30]A. Dmitriev and M. Dyakonov, Sov. Phys. JETP **63**, 838 (1986).